# Isotope effect of Co diffusion in amorphous $Co_{76.7}Fe_2Nb_{14.3}B_7$

P. W. Hüppe and F. Faupel
*Institut für Metallphysik, Abteilung Metallkunde, Hospitalstrasse 3-7, D-3400 Göttingen, Federal Republic of Germany*
(Received 30 September 1991)

Utilizing the radiotracers $^{57}Co$ and $^{60}Co$, we have investigated the isotope effect of Co diffusion in melt-spun amorphous $Co_{76.7}Fe_2Nb_{14.3}B_7$ between 626 and 642 K. The ion-beam sputtering technique was employed for serial sectioning. For comparison, measurements were also carried out in fcc Co at 1049 K. The resulting isotope effect $E \equiv (D_\alpha/D_\beta - 1)/[(m_\beta/m_\alpha)^{1/2} - 1] = 0.74 \pm 0.05$ in polycrystalline Co is typical of diffusion via monovacancies in densely packed structures. In contrast, the extremely small value of $E = 0.1 \pm 0.01$ obtained in amorphous $Co_{76.7}Fe_2Nb_{14.3}B_7$ allows us to rule out a defect-mediated single-atomic-jump mechanism and is consistent with a diffusion mechanism involving about ten atomic masses.

## INTRODUCTION

Diffusion in crystalline metals and substitutional alloys is generally mediated by point defects.[1] Arrhenius plots (logarithm of diffusivity $D$ vs inverse absolute temperature $T$) are linear over many decades. In some cases a slight curvature has been observed at high temperatures[2] and attributed to the contribution of divacancies. The activation energy for diffusion consists of the energies of vacancy formation and migration. The activation volume, which can be determined from the pressure dependence of diffusion,[3] is of the order of a relaxed vacancy volume. Measurements of the isotope effect have shown that diffusion takes place by single-atom jumps into vacancies. In close-packed structures, about 90% of the kinetic energy at the saddle point resides in the jumping atom.[1]

In metallic glasses (hereafter also termed amorphous alloys) our present knowledge of the diffusion mechanisms is rather limited, despite more than 15 years of research.[4-10] On the other hand, the stability of metallic glasses with respect to structural relaxation, phase separation, and crystallization is controlled by diffusion processes. Diffusion also plays a role in amorphization by solid-state reaction of thin films and in ball milling.[11-13]

Structural relaxation is most pronounced in melt-spun glasses and leads to a drop in the diffusivity due to annealing of excess volume but it approaches a final value which represents the fully relaxed metastable amorphous state.[14-16] Reproducible results can only be expected if diffusion measurements are carried out in this state, which was not the case in many of the earlier investigations. The onset of crystallization restricts the maximum annealing temperature and time to values corresponding to a typical diffusion length of some 10 nm.

All reliable measurements, in particular those carried out using radiotracers and direct high-resolution depth profiling, clearly show that diffusion in metallic glasses also follows an Arrhenius type of behavior with constant activation energy $Q$ and a preexponential factor $D_0$, typical of thermally activated processes (see Refs. 8–10 for recent reviews). This suggests a relatively sharp distribution of activation energies. Kronmüller and Frank,[17] assuming a Gaussian distribution of activation energies, came to the conclusion that, in view of the narrow temperature range which is accessible and the experimental error of the diffusion constants, the data are compatible with half-widths of the activation energy spectra of about 0.3 eV.

Several experimental observations, including radiation-enhanced diffusion,[18,19] void formation,[20] and the pressure dependence of the crystallization kinetics,[21] have been considered as evidence of diffusion via point defects in thermal equilibrium.

On the other hand, preexponential factors determined from Arrhenius plots exhibit an extreme variability over more than 10 orders of magnitude,[17] which does not appear to be consistent with a vacancylike mechanism of diffusion. Alternatively, it has been suggested that diffusion in metallic glasses takes place by cooperative mechanisms.[5,16,22-24]

Recently, we have investigated a pressure dependence of $^{60}Co$ self-diffusion in structurally relaxed amorphous $Co_{76.7}Fe_2Nb_{14.3}B_7$ (Refs. 25 and 26) and in fcc Co (Ref. 27) by means of a direct radiotracer technique in conjunction with ion-beam sputtering (IBS) for microsectioning. While an activation volume of the order of a relaxed vacancy volume was found in fcc Co, no pressure dependence could be resolved in the metallic glass. This allowed us to rule out thermal-equilibrium vacancies as a diffusion mechanism. Diffusion can either occur via athermal vacancylike entities or by means of a direct cooperative mechanism, i.e., without any assistance of defects.

In the present paper, we report the isotope-effect measurements of Co diffusion in the $Co_{76.7}Fe_2Nb_{14.3}B_7$ glass that was also used for studying the pressure dependence. These results have been presented by us recently.[25] In view of the close similarity between Co and Fe and the small Fe content, this material can be regarded as a ternary cobalt-rich Co-Nb-B alloy, at least with respect to diffusion. Since, for a cooperative diffusion mechanism, a large number of atoms should participate in the diffusive jump, an extreme "dilution" of the isotope effect is to be

 

expected. We shall see that this is indeed the case for Co diffusion in the amorphous alloy. In order to demonstrate the reliability of the radiotracer technique utilized in this work, the isotope effect was measured in fcc Co at 1049 K, too. At this temperature the penetration depths of the two tracers in Co and in the metallic glass are comparable.

## EXPERIMENTAL

Melt-spun amorphous $Co_{76.7}Fe_2Nb_{14.3}B_7$ ribbon of 70 $\mu$m thickness and 20 mm width was kindly provided by Vacuumschmelze Hanau, FRG. The ribbon was characterized by means of differential scanning calorimetry, electron microprobe analysis, and x-ray diffraction prior to and after the diffusion anneals. Measurements of the coercive field were carried out by the manufacturer. Details are given in Ref. 26.

Samples of 12 mm diameter were punched out of the relatively brittle amorphous ribbon. The specimens were preannealed at 690 K, well below the crystallization temperature of 743 K, for 360 min. After this heat treatment the material proved to be in the structurally relaxed metastable state as evidenced by a time-independent diffusivity.[26]

For precise measurements of the isotope effect, a high-surface finish of the specimens is essential. Melt-spun amorphous ribbons generally exhibit a shiny side and a dull one, which was exposed to the rotating copper wheel. The shiny surface of the Co-Fe-Nb-B glass had a wavy structure. Amplitude and wavelength in the $\mu$m and mm range, respectively, were much too large to affect depth profiling on a 10-nm scale. Prior to evaporation of the tracers, different cleaning procedures were tested. Direct deposition of the tracer resulted in a strong perturbation of the penetration profile due to surface oxidation and/or crystallization over a distance of about 50 nm as shown in Fig. 1. Mechanical and chemical polishing lead to improvements. However, we obtained best results for both sides of the ribbon by sputter cleaning with 600-eV argon ions removing a surface layer of $\approx$90 nm thickness (Fig. 1). The preparation of the cobalt samples has been described elsewhere.[27]

Carrier-free $^{57}$Co and $^{60}$Co isotops obtained in a 0.1-m HCl solution from Amersham Buchler were employed as tracers. During flash evaporation in high vacuum, CoCl was thermally decomposed and typically 100 kBq ($\simeq$3 $\mu$Ci) of a mixture of $^{60}$Co and $^{57}$Co were deposited on the sample. The ratio of $^{60}$Co to $^{57}$Co was chosen to yield optimal count rates in the Ge detector (see below). The thickness of the tracer layer was of the order of one monolayer. Under these conditions, the thin-film solution of Fick's second law[1] could be applied for the evaluation of diffusion constants in all cases. A mask was used to avoid contamination of the sample edges which could lead to severe artifacts in depth profiling.

The samples were annealed in a vacuum of 0.1 Pa for 360–820 min. The temperature of the furnace was controlled within $\pm$1 K. Afterwards no indications of crystallization or oxidation could be detected by means of sensitive x-ray measurements.[26]

Serial sectioning was performed in a dc ion-beam sputtering apparatus with a duoplasmatron-type of ion source.[28] The specimen was mounted on a motor-driven copper holder (ca. 1 rpm). It was attached by means of a small short-circuited magnet. The embedded magnet had no influence on the homogeneity of the sputter rate ($<\pm$3%).

Usually in IBS a graphite cap is used to protect the sample holder and other components from the ion beam. However, graphite, due to its extremely low sputter yield and porous surface, was found to store a small portion of activity, particularly from the very active near-surface layers. This activity is then sputtered off again and gives rise to a time-dependent background, which reduces depth resolution and sensitivity.[28] This background was determined by removing the active sample from the holder and resuming the sputter process. Figure 2 clearly demonstrates that the aftereffect is largely reduced by usage of a plain Cu sample holder without graphite cap. The influence of the sputter background correction on a

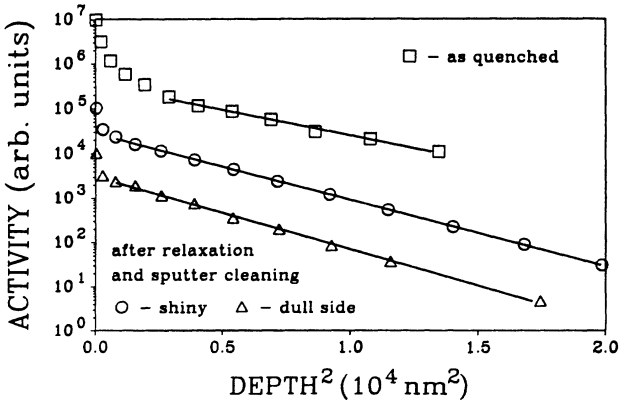


FIG. 1. Penetration profiles of $^{60}$Co into amorphous Co-Fe-Nb-B ribbon obtained as quenched and after relaxation and removal of a 90-nm surface layer from the shiny and dull side. The dull side was in contact with the copper wheel during melt-spinning. The annealing time and temperature were 360 min and 677 K, respectively.

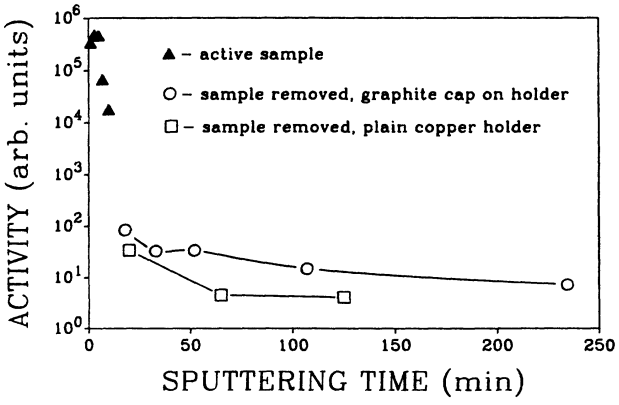


FIG. 2. Aftereffect in ion-beam depth profiling due to sputtering of activity spread onto components other than the catcher foil.

representative penetration profile is displayed in Fig. 5. While the background correction does not change the slope of the profile significantly and can therefore be neglected in many applications, its proper determination and subtraction proved to be necessary to achieve the high precision required in the present isotope-effect measurements.

Sputtering was performed with 600-eV $Ar^+$ ions. The beam current, of the order of 0.5 mA/cm$^2$, was kept constant electronically within $<\pm 0.5\%$. The sputtering rate ($\approx 3$ nm/min) was determined from the total weight loss (typical 200 $\mu$g), the cross-sectional area, the density of the specimen, and the sputtering time. The weight loss was measured with a microbalance of 1-$\mu$g resolution. A density of $8.4\pm 0.2$ g/cm$^3$ was calculated from Vegard's rule, which is well obeyed in metallic glasses.[29] The same density was evaluated from measurements of volume and mass. Slight uncertainties in the density only introduce a corresponding error into the preexponential factor $D_0$ of diffusion. However, this error is negligible compared to the experimental uncertainty of $D_0$. The material removed by sputtering was collected on a Mylar foil (Du-

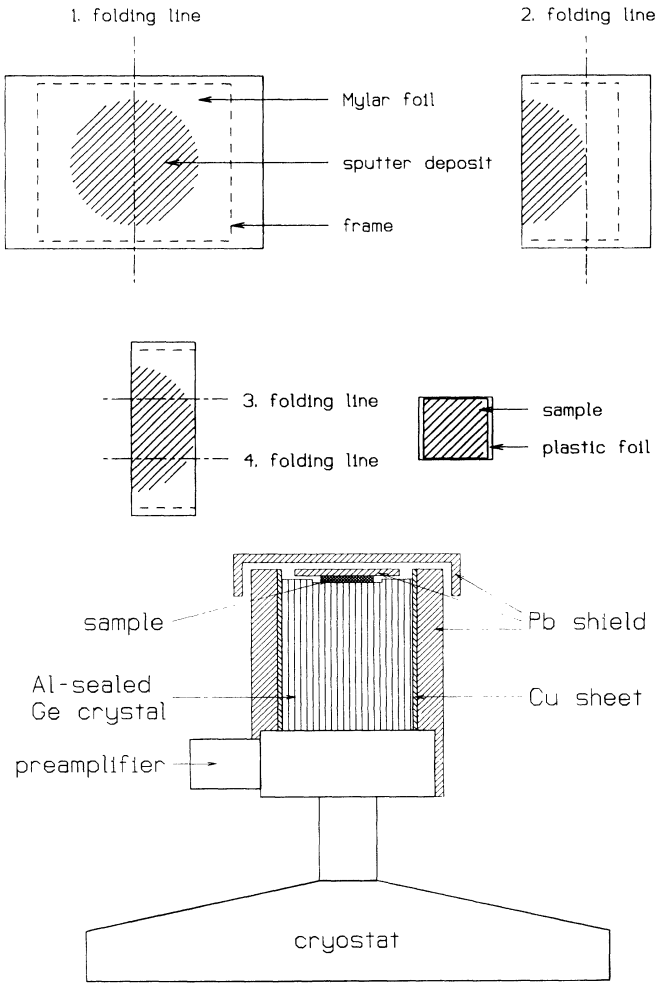


FIG. 3. Reproducible preparation of an active Mylar foil section (top) and sketch of the setup utilized for $\gamma$ counting by means of a high-resolution intrinsic Ge detector (bottom).

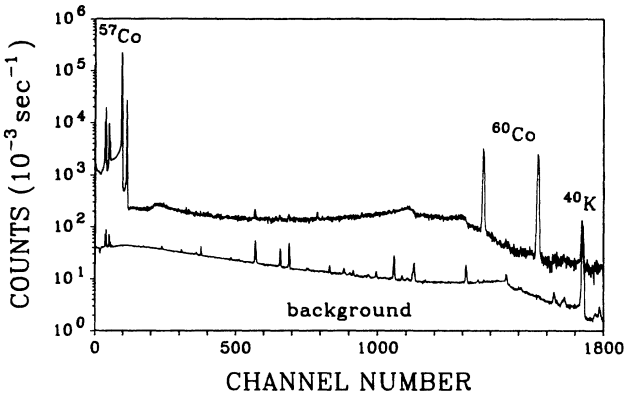


FIG. 4. Typical $\gamma$ spectrum on a semilogarithmic scale.

Pont) which was quickly advanced after each section by means of a computer-controlled motor without interrupting the sputtering process. Subsequently, the film was cut into rectangular pieces corresponding to individual sections, which could be easily identified as spots. In order to assure constant counting geometry, the Mylar foil was folded in a reproducible manner as illustrated in Fig. 3, sealed in a plastic foil for protection, and placed inside the detector in a well-defined geometry (Fig. 3).

The high-resolution intrinsic 106-cm$^3$ Ge detector (Princeton Gamma-Tech.) was shielded with lead (wall thickness 8 mm) and copper for background reduction. It was connected to a preamplifier and a computer controlled multichannel analyzer (EG&G Ortec). A typical spectrum is depicted in Fig. 4. The $^{60}$Co 1.173- and 1.332-MeV and $^{57}$Co 122- and 136-keV $\gamma$ lines were used for counting. The efficiency of the detector was higher by a factor of about 20 for the low-energy $^{57}$Co lines. This was partly compensated by a correspondingly higher concentration of $^{60}$Co in the mixture of tracers. A complete compensation is not useful because of the influence of the linear $^{60}$Co background in the range of the $^{57}$Co peak. The absorption mean free path for the $^{60}$Co radiation in Ge is much larger than the radius of the detector crystal. In this energy range the wall thickness of a $4\pi$ detector enters exponentially into the counting efficiency. This was the main reason for utilizing a detector with $2\pi$ rather than well-type geometry. For the isotope-effect measurements, the ratio of the $^{57}$Co and $^{60}$Co activity has to be independent of the count rate. As shown in Fig. 6, this null effect is negligible in the activity range employed in the present investigation.

## RESULTS

Penetration profiles of $^{60}$Co into amorphous Co-Fe-Nb-B and fcc Co are depicted in Figs. 1 and 5. According to the thin-film solution of Fick's second law,[1]

$$c(x)=\text{const}\exp(-x^2/4Dt)\ , \tag{1}$$

the activity, which is proportional to the tracer concentration $c$, is plotted versus the square of the penetration depth $x$. Straight lines were fitted to the data. The

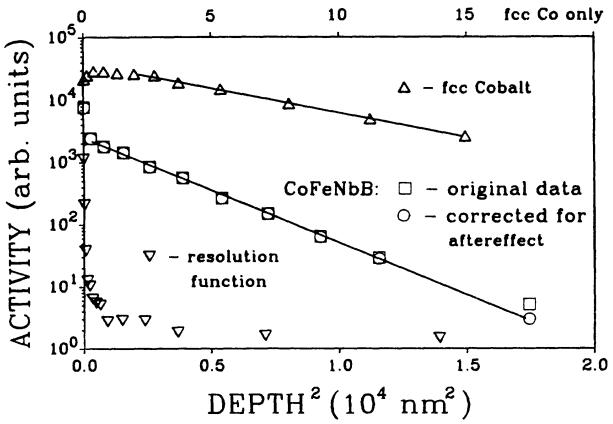


FIG. 5. Penetration profiles of $^{60}$Co into amorphous Co-Fe-Nb-B and fcc Co, together with the resolution function of the present IBS technique. The profile obtained in the amorphous Co-Fe-Nb-B is also shown prior to correction for the aftereffect (see text). The annealing times and temperatures were 370 min at 666 K and 810 min at 1049 K for Co-Fe-Ni-B (unrelaxed) and fcc Co, respectively.

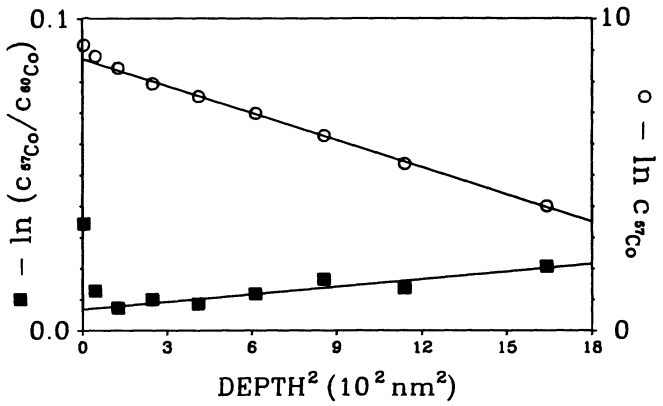


FIG. 7. Semilogarithmic penetration profile of $^{57}$Co (right-hand scale) and ratio of the $^{57}$Co and $^{60}$Co activities (left-hand scale) vs the square of the penetration depth for diffusion in amorphous $Co_{76.7}Fe_2Nb_{14.3}B_7$. For illustration, the square of the penetration depth, which is proportional to ln$c$, was chosen as common abscissa. The sample was annealed at 642 K for 750 min.

diffusivity $D$ can be extracted from the slope and the annealing time $t$. The resolution function of the present microsectioning technique, i.e., the profile of a sample not subjected to heat treatment, is also shown in Fig. 5. In contrast to depth profiling by means of secondary ion mass spectrometry, which involves ion energies in the keV range, the limitations of depth resolution can be neglected here. As illustrated in Fig. 1, the diffusivities determined at the dull and shiny sides of the amorphous ribbon are identical within experimental error in samples which were preannealed to promote structural relaxation. This is an additional indication that the experiments were carried out in the well-defined metastable state.

The temperature dependence of Co tracer diffusion in amorphous $Co_{76.7}Fe_2Nb_{14.3}B_7$ has been reported in Ref. 25. A linear relationship between ln$D$ and $1/T$ with an activation energy of $2.3\pm0.2$ eV and a preexponential factor of $D_0 = 1\times10^{-3}$ m$^2$/s was observed.

It follows from Eq. (1) that the mass effect of diffusion $D_\alpha/D_\beta - 1$ can be determined directly by plotting $\ln(c_\alpha/c_\beta)$ against $\ln c_\alpha$. Corresponding graphs are depicted in Fig. 6 for crystalline Co and the metallic glass.

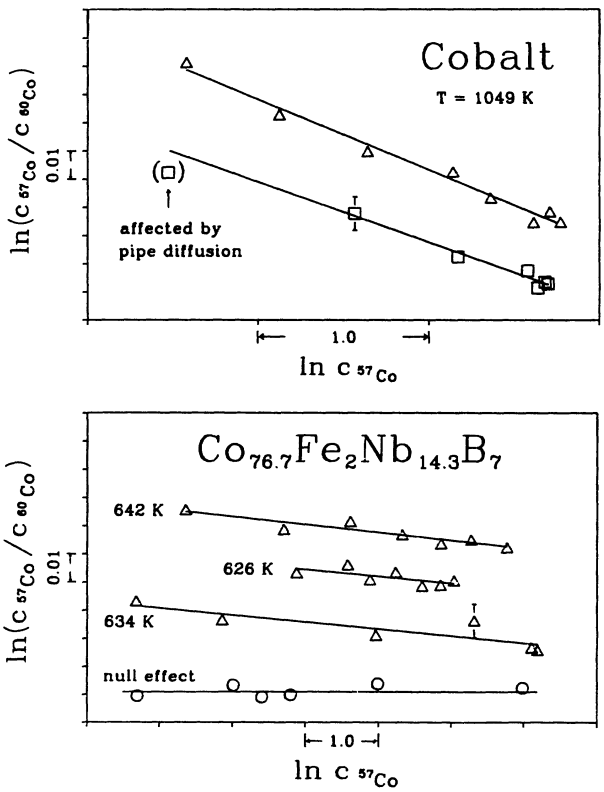


FIG. 6. Logarithmic plot of the $^{57}$Co and $^{60}$Co activity ratio as function of the $^{57}$Co activity for diffusion in fcc Co and the metallic glass $Co_{76.7}Fe_2Nb_{14.3}B_7$. The slope of the straight lines directly yields $D_{57}/D_{60} - 1$. The null effect of the detector is shown, too.

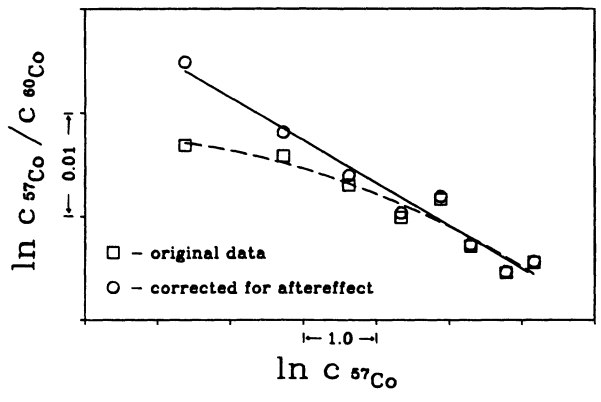


FIG. 8. Logarithmic plot of the $^{57}$Co and $^{60}$Co activity ratio vs $^{57}$Co activity for diffusion in amorphous $Co_{76.7}Fe_2Nb_{14.3}B_7$. Data corrected for the aftereffect in ion-beam sputtering and original values are displayed. This plot is based on the same measurement as the one shown in Fig. 7.

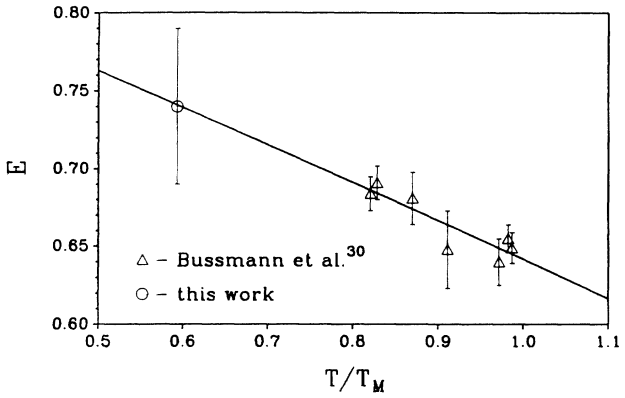


FIG. 9. Isotope effect of self-diffusion in fcc Co as a function of temperature.

From the slopes the following isotope effects

$$E \equiv (D_{57}/D_{60}-1)/[(m_{60}/m_{57})^{1/2}-1] \quad (2)$$

were obtained: $E=0.74\pm0.05$ in fcc Co and $E=0.1\pm0.01$ in amorphous $Co_{76.7}Fe_2Nb_{14.3}B_7$. The susceptibility of the isotope-effect evaluation to small deviations from the linear range of penetration profiles is elucidated in Fig. 7. Only data points from the linear range are plotted in Fig. 6. The deviations from linearity for fcc Co are due to short-circuit diffusion mainly along grain boundaries.[27,30] Figure 8 demonstrates the necessity of aftereffect corrections.

The diffusion constant of $D=(3.3\pm0.5)\times10^{-15}$ cm$^2$/s obtained for fcc Co at 1049 K agrees well with measurements of Bussmann *et al.*[30] The present isotope-effect value is also in good accord with a linear extrapolation of $E(T)$ data determined at higher temperatures by these authors. Apparently, our measuring technique allows us to determine reliable isotope effects (Fig. 9).

## DISCUSSION

For self-diffusion in fcc Co, a vacancy mechanism is well established.[1,30] At low temperatures only monovacancies are responsible for diffusion. This is also reflected in the activation volume of 0.71 atomic volume.[27] The mass effect can be written as[31,32]

$$\frac{D_\alpha}{D_\beta}-1=\left[\left(\frac{m_\beta+(n-1)m}{m+(n-1)m}\right)^{1/2}-1\right]f\Delta K \ . \quad (3)$$

Here $m_i$ are the masses of the isotopes, $m$ is the average mass of the matrix, $n$ is the number of atoms that migrate simultaneously, and $f$ is the correlation factor. $\Delta K$ is the fraction of kinetic energy associated with motion parallel to the jump direction in the saddle-point configuration which resides in the $n$ jumping atoms. (Strictly speaking, "parallel" refers to configuration space.) $\Delta K$ accounts for many-body effects.

For self-diffusion via monovacancies $n=1$ and $f$ solely depends on the lattice geometry. For fcc crystals $f=0.782$.[1] From our isotope-effect result we then obtain $\Delta K=0.95$ at 1049 K. This value reflects that only a very small fraction of kinetic energy is transferred to neighboring atoms during a jump. $\Delta K$ is always found to be close to unity for a monovacancy mechanism in dense structures.[1]

In contrast, the extremely small isotope effect of $E=0.1$ measured in amorphous $Co_{76.7}Fe_2Nb_{14.3}B_7$ is inconsistent with an indirect diffusion mechanism via vacancylike entities. For a vacancy mechanism, the many-body factor $\Delta K$ should be larger than 0.5.[33] The correlation factor, to a crude approximation, can be estimated from the probability of a reverse jump of the tracer into the defect and thus from the number of nearest-neighbor atoms which compete for the vacancy.[34] Therefore, the hypothetical correlation factor for Co diffusion in the Co-rich glass should not deviate drastically from the correlation factor for self-diffusion and, hence, cannot account for an isotope effect as low as 0.1.

In this light we attribute the extremely small mass effect to the participation of a large number of atoms in the jump process and consider a direct diffusion mechanism without assistance of any defects and $f=1$. If the correlation factor $f$ equals unity, the restrictions usually concomitant with the validity of Eq. (3) (Ref. 34) for $f\neq1$ do not apply. Consequently, it should be possible to get at least a rough estimate of the number of atoms that are involved in a jump from Eq. (3).

Whether the weak isotope effect is essentially due to a large $n$ in Eq. (3) or a small $\Delta K$ cannot be concluded definitely from the measurements. Both descriptions are complementary to a certain extent since, in both cases, $E$ is strongly reduced by participation of a large number of atoms in the jump.

Two extreme conditions can be considered. A lower bound of $n\simeq10$ is obtained by putting $\Delta K=1$ and attributing the whole effect to $n$. This essentially corresponds to simultaneous motion of $n$ atoms, all contributing equally to the diffusion process. Presumably, however, $n$ is very much a weighted-average quantity involving some ten atoms.

One might also consider the other extreme of a single-jump mechanism where $n=1$ and $\Delta K\ll1$. Within this framework, the jump of the tracer is initiated by fluctuations, and a hole, large enough for the tracer to jump in, is created by strong displacements of the surrounding atoms opposite to the jump direction. After the jump process, the structure is completely relaxed. It is evident that the larger the relaxation of neighboring atoms, the greater may be their motion and the more removed will $\Delta K$ be from unity. Le Claire[34] has established a very rough quantitative connection between $\Delta K$ and the volume $\Delta V$ remaining after relaxation:

$$\Delta K=\frac{1}{1+(N/3)|1-\Delta V|} \ . \quad (4)$$

Here $N$ is the number of atoms that contribute to the relaxation. With $\Delta K=0.1$ and $\Delta V=0$, one obtains $N\simeq30$ in good accord with the above estimate.

## SUMMARY

We have measured the isotope effect of $^{57}$Co and $^{60}$Co diffusion in crystalline fcc Co and in structurally relaxed

melt-spun amorphous $Co_{76.7}Fe_2Nb_{14.3}B_7$. Microsectioning was carried out by means of ion-beam sputtering. Based on an elaborated surface treatment of the amorphous ribbon and careful consideration and reduction of sputter artefacts, it was possible to determine reliable isotope-effect values. In crystalline Co a large isotope effect, typical of diffusion via single-atom jumps into vacancies, was obtained. In contrast, the resulting extremely small isotope effect in the metallic glass is inconsistent with diffusion via vacancylike defects. It rather points to a strong "dilution" of the mass effect through participation of a large number of atoms in the elementary diffusive jump. Within this framework, our measurements suggest the involvement of about ten atomic masses.

## ACKNOWLEDGMENTS

We are indebted to K. Rätzke and Th. Hehenkamp for stimulating discussions and critically reading the manuscript. The amorphous samples were kindly provided by Vacuumschmelze Hanau. Part of this work has been supported by Deutsche Forschungsgemeinschaft under Grant No.Fa 234/1-1.

[1]Y. Adda and J. Philibert, *La Diffusion dans les Solides* (Press Universitaires de France, Paris, 1966).

[2]A. Seeger and H. Mehrer, in *Vacancies and Interstitials in Metals,* edited by A. Seeger, D. Schumacher, W. Schilling, and J. Diehl (North-Holland, Amsterdam, 1970), p. 1.

[3]D. Lazarus, in *DIMETA 82,* edited by F. J. Kedves and D. L. Beke (Trans. Tech., Aedermannsdorf, 1983), p. 134.

[4]D. Gupta, K. N. Tu, and K. W. Asai, Phys. Rev. Lett. **35**, 796 (1975).

[5]B. Cantor and R. W. Cahn, in *Amorphous Metallic Alloys,* edited by F. E. Luborsky (Butterworth's, London, 1983), p. 487.

[6]B. Cantor, in *Proceedings of the 5th International Conference on Rapidly Quenched Metals,* edited by S. Steeb and H. Warlimont (North-Holland, Amsterdam, 1985), p. 595, and references therein.

[7]J. Horváth, K. Pfahler, W. Ulfert, W. Frank, and H. Mehrer, J. Phys. C. **8**, 645 (1985).

[8]Y. Adda, G. Brebec, R. P. Gupta, and Y. Limoge, Mater. Sci. Forum **15-18**, 349 (1987).

[9]H. Mehrer and W. Dörner, Defect Diffus. Forum **66-69**, 189 (1989).

[10]Y. Limoge, in *Diffusion in Materials,* Vol. 169 of *NATO Advanced Study Institute Series E,* edited by A. C. Laskar, J. L. Bocquet, G. Brebec, and C. Monty (Plenum, New York, 1990), p. 601.

[11]X. L. Yeh, K. Samwer, and W. L. Johnson, Appl. Phys. Lett. **42**, 242 (1983).

[12]R. B. Schwarz and W. L. Johnson, Phys. Rev. Lett. **51**, 415 (1983).

[13]A. Y. Yermakov, Y. Y. Yurchikov, and V. A. Barinov, Phys. Met. Metall. **52**, 50 (1981).

[14]H. S. Chen, L. C. Kimerling, J. M. Poate, and W. L. Brown, Appl. Phys. Lett. **32**, 461 (1978).

[15]J. Horváth, K. Pfahler, W. Ulfert, W. Frank, and H. Kronmüller, Mater. Sci. Forum **15-18**, 523 (1987).

[16]W. Frank, J. Horváth, and H. Kronmüller, Mater. Sci. Eng. **97**, 415 (1988).

[17]H. Kronmüller and W. Frank, Radiat. Eff. Defects Solids **108**, 81 (1988).

[18]R. S. Averback and H. Hahn, Phys. Rev. B **37**, 10 383 (1988).

[19]A. K. Tyagi, M. P. Macht, and V. Naundorf, J. Nucl. Mater. **179-181**, 1026–1029 (1991).

[20]K. N. Tu and T. C. Chou, Phys. Rev. Lett. **61**, 1863 (1988).

[21]Y. Limoge, J. Non Cryst. Solids **117/118**, 708 (1990).

[22]E. Stelter and D. Lazarus, Phys. Rev. B **36**, 9545 (1987).

[23]D. Lazarus, in *Phase Transition in Condensed Systems,* edited by C. G. Cargill, F. Spaepen, and K. Tu, MRS Symposia Proceedings No. 57 (Materials Research Society, Pittsburgh, 1987), p. 297.

[24]F. Spaepen, in *Physics of Defects,* Proceedings of the Les Houches Summer School Session XXXV, 1980, edited by R. Balian and W. Kléman (North-Holland, Amsterdam, 1981), p. 136.

[25]F. Faupel, P. W. Hüppe, and K. Rätzke, Phys. Rev. Lett. **65**, 1219 (1990).

[26]K. Rätzke and F. Faupel, Phys. Rev. B **45**, 7459 (1992).

[27]K. Rätzke and F. Faupel, Scr. Metall. **25**, 2233 (1991).

[28]F. Faupel, P. W. Hüppe, K. Rätzke, R. Willecke, and Th. Hehenkamp, I. Vac. Sci. Technol. (A)**10**, 92 (1992).

[29]K. Aso, M. Hayakawa, K. Hotai, S. Kedaira, Y. Ochiai, and Y. Makino, in *Proceedings of the 4th International Conference on Rapidly Quenched metals, Sendai, 1981,* edited by U. Suzuki and T. Masumoto (Japan Institute of Metals, Sendai, 1982), p. 379.

[30]W. Bussmann, C. Herzig, W. Rempp, K. Maier, and H. Mehrer, Phys. Status Solidi **56**, 87 (1979).

[31]J. G. Mullen, Phys. Rev. **121**, 1649 (1961).

[32]A. D. Le Claire, Philos. Mag. **14**, 127 (1966).

[33]R. C. Brown, J. Worster, N. H. March, R. C. Perrin, and R. Bullough, Philos. Mag. **23**, 555 (1971).

[34]A. D. Le Claire, in *Physics and Chemistry, An Advanced Treatise,* edited by W. Jost (Academic, New York, 1970), Vol. 10, p. 261.